Article

Dead-End Street of Protein Folding: Thermodynamic Rationale of Amyloid Fibril Formation

Andrs Perczel, Pter Hudky, and Vill K. Plfi

J. Am. Chem. Soc., **2007**, 129 (48), 14959-14965 • DOI: 10.1021/ja0747122

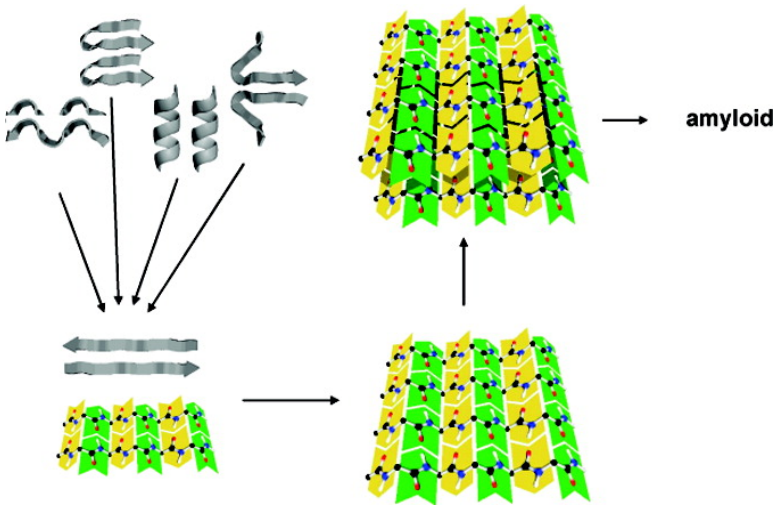

More About This Article

Additional resources and features associated with this article are available within the HTML version:

- Supporting Information
- Links to the 6 articles that cite this article, as of the time of this article download
- Access to high resolution figures
- Links to articles and content related to this article
- Copyright permission to reproduce figures and/or text from this article

View the Full Text HTML

J|A|C|S
ARTICLES
Published on Web 11/13/2007

Dead-End Street of Protein Folding: Thermodynamic Rationale of Amyloid Fibril Formation

András Perczel,*[,†,‡] Péter Hudáky,[‡] and Villö K. Pálfi[†]

Contribution from the Laboratory of Structural Chemistry and Biology, Institute of Chemistry, Eötvös Loránd University, Pázmány Péter sétány 1/A, H-1117, Budapest, Hungary, and Protein Modeling Group HAS-ELTE, Institute of Chemistry, Eötvös Loránd University, H-1538, Budapest, P.O.B. 32, Hungary

Received June 27, 2007; E-mail: perczel@chem.elte.hu

Abstract: An increasing number of diseases, including Alzheimer's, have been found to be a result of the formation of amyloid aggregates that are practically independent of the original primary sequence of the protein(s). (Eakin, C. M.; Berman, A. J.; Miranker, A. D. *Nat. Struct. Mol. Biol.* **2006**, *13*, 202−208.) Consequently, the driving force of the transformation from original to disordered amyloid fold is expected to lie in the protein backbone, which is common to all proteins. (Nelson, R.; Sawaya, M. R.; Balbirnie, M.; Madsen, A. O.; Riekel, C.; Grothe, R.; Eisenberg, D. *Nature* **2005**, *435*, 773−778. Wright, C. F.; Teichmann, S. A.; Clarke, J.; Dobson, C. M. *Nature* **2005**, *438*, 878−881.) However, the exact explanation for the existence of such a "dead-end" structure is still unknown. Using systematic first principle calculations on carefully selected but large enough systems modeling the protein backbone we show that the β-pleated sheet structure, the building block of amyloid fibers, is the thermodynamically most stable supramolecular arrangement of all the possible peptide dimers and oligomers both in vacuum and in aqueous environments. Even in a crystalline state (periodical, tight peptide attechment), the β-pleated sheet assembly remains the most stable superstructure. The present theoretical study provides a quantum-level explanation for why proteins can take the amyloid state when local structural preferences jeopardize the functional native global fold and why it is a β-pleated sheetlike structure they prefer.

Introduction

The primary sequence of a globular protein encodes its three-dimensional structure related to its biological function.[1] However, growing evidence supports that an alternative, well organized, but different 3D structure could exist for many proteins.[2] Dozens of ordinary proteins (e.g., SH3, β-2 microglobulin, lysozyme, myoglobin)[3,4] tend to aggregate if misfolded in abnormal cellular conditions,[5] showing an architecture similar to that of the amyloid peptide, which is responsible for the development of Alzheimer's disease.[6] The conversion from the globular form into an amyloid-like aggregate is the transformation of the physiologically "healthy" structure into a nonfunctional, pathogenic conformer. Thus, understanding the molecular mechanisms of such a transformation and deciphering the underlying thermodynamic cause has wide ranging applications.

Amyloid and other threadlike aggregates share the common building motif of multiple stranded β-pleated sheets.[2,7,8,9] In the correct conditions, practically any protein investigated could be trapped in a toxic β-layer form.[2,10,11,12] Thus, the folding propensities encoded by the protein side chains have apparently little or no impact on the formation of the aggregate.[3,13,14] Also, as a recently proposed backbone-based theory of protein folding emphasizes, the energetics of backbone hydrogen bonds dominate the overall folding process[15] even for "normally" folded proteins. Thus, strong backbone−backbone interactions (primarily interchain hydrogen bonds) that are well pronounced in β-strands are expected to be the driving force of amyloid-like aggregation, leading to a folding dead-end.

In this work the following three issues are addressed: (*i*) the stability of β-strand aggregates relative to other secondary structure elements (e.g., aggregates of helices), (*ii*) why β-strand aggregates are thermodynamically preferred, and (*iii*) how compact is a lattice or matrix formed from aggregates of β-strands.

[†] Laboratory of Structural Chemistry and Biology.
[‡] Protein Modeling Group HAS-ELTE.

(1) Anfinsen, C. B. *Nature* **1973**, *181*, 223−230.
(2) Nelson, R.; Sawaya, M. R.; Balbirnie, M.; Madsen, A. O.; Riekel, C.; Grothe, R.; Eisenberg, D. *Nature* **2005**, *435*, 773−778.
(3) Dobson, C. M. *Trends Biochem. Sci.* **1999**, *24*, 329−332.
(4) Fandrich, M.; Forge, V.; Buder, K.; Kittler, M.; Dobson, C. M.; Diekmann, S. *Proc. Natl. Acad. Sci. U.S.A.* **2003**, *100*, 15463−15468.
(5) Dobson, C. M. *Nat. Struct. Mol. Biol.* **2006**, *13*, 295−297.
(6) Dobson, C. M. *Nature* **2005**, *435*, 747−749.
(7) Sunde, M.; Blake, C. *Adv. Protein Chem.* **1997**, *50*, 123−159.
(8) Nelson, R.; Eisenberg, D. *Curr. Opin Struct. Biol.* **2006**, *16*, 260−265.
(9) Chan, J. C. C.; Oyler, N. A.; Yau, W. M.; Tycko, R. *Biochemistry-Us* **2005**, *44*, 10669−10680.
(10) Eakin, C. M.; Berman, A. J.; Miranker, A. D. *Nat. Struct. Mol. Biol.* **2006**, *13*, 202−208.
(11) Jimenez, J. L.; Nettleton, E. J.; Bouchard, M.; Robinson, C. V.; Dobson, C. M.; Saibil, H. R. *Proc. Natl. Acad. Sci. U.S.A.* **2002**, *99*, 9196−9201.
(12) Guijarro, J. I.; Sunde, M.; Jones, J. A.; Campbell, I. D.; Dobson, C. M. *Proc. Natl. Acad. Sci. U.S.A.* **1998**, *95*, 4224−4228.
(13) Fandrich, M.; Dobson, C. M. *EMBO J.* **2002**, *21*, 5682−5690.
(14) Chiti, F.; Stefani, M.; Taddei, N.; Ramponi, G.; Dobson, C. M. *Nature* **2003**, *424*, 805−808.
(15) Rose, G. D.; Fleming, P. J.; Banavar, J. R.; Maritan, A. *Proc. Natl. Acad. Sci. U.S.A.* **2006**, *103*, 16623−16633.

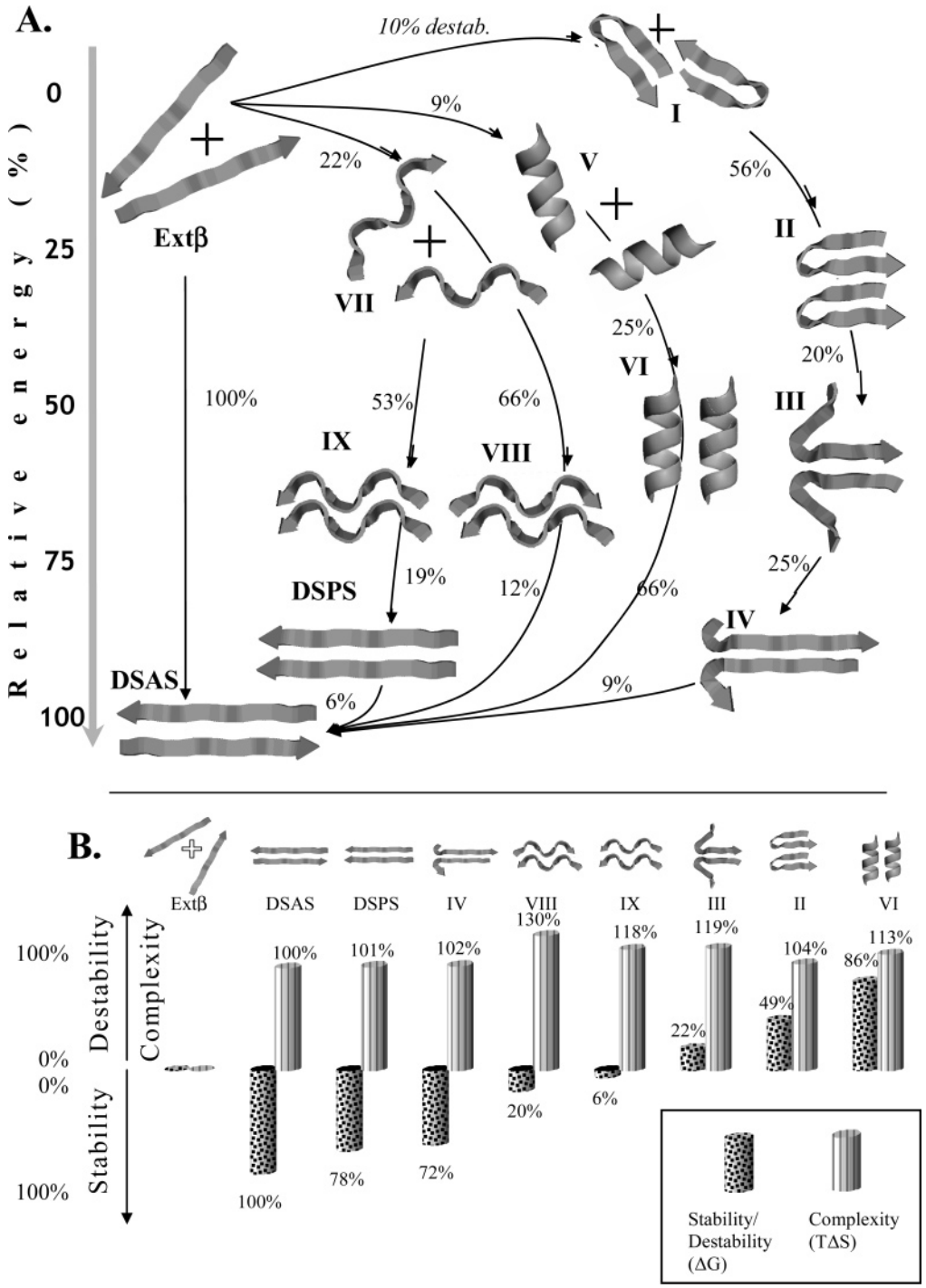

Figure 1. (A) Relative stability (ΔE in %) of a folding or aggregation step of short polypeptides with respect to the formation of a DSAS, from its isolated Extβ units (detailed data shown in Table 1 and Table S1). Arrows connect selected intermediate conformers that are prevalent during the folding of proteins. (B) Complexity, $-T\Delta S$, and stability (or destability), ΔG, measured in the hydrophobic environment ($\epsilon = 1$) of different secondary structure dimers. A 100% of entropy change at 300 K and 100% of stability increase, ΔG, are related to the formation of the DSAS from two Extβ (for more details see Table S1). Roman numbers and abbreviations denote the following structures: Extβ: (I) hairpin with type II β-turn, (II) hairpin dimer of type II β-turns, (III) intermediate structure, (IV) DSAS with open ends, (V) single 3_{10} helix, (VI) 3_{10} helix dimer, (VII) repeated inverse γ-turns, (VIII) antiparallel repeated inverse γ-turns, (IX) parallel repeated inverse γ-turns; DSPS: *d*ouble *s*tranded *p*arallel β-sheet.

The present study provides theoretical calculations on carefully selected model systems to explore the thermodynamics of amyloid formation. First principle calculations using relatively small and simplified peptide models have already proved to reproduce the thermodynamic behavior of larger systems and correlate with experimental structural data and so providing theoretical explanation for several aspects of the protein folding problem.[16,17,18]

Model selection for this study is also justified by the observation that aggregates are typically formed from protein

(16) Perczel, A.; Angyan, J. G.; Kajtar, M.; Viviani, W.; Rivail, J. L.; Marcoccia, J. F.; Csizmadia, I. G. *J. Am. Chem. Soc.* **1991**, *113*, 6256−6265.

fragments (e.g., Aβ 1−42 and 6 residues long peptides[19]) and the consideration that dimerization can be regarded as the minimal model of aggregation.

Methods

For all calculations the Gaussian03[20] software program was used. Di-, tetra-, hexa-, and octapeptides and their aggregates {For-(L-Ala)$_i$-NH$_2$}$_j$ where i = 2, 4, 6, 8.. and j = 1, 2, 3, 4,..} in a hydrophobic environment (ϵ = 1) were fully geometry optimized at the B3LYP/6-31G(d) level of theory. For all optimized tetrapeptides and selected additional models, frequency calculations (vibrational analysis) were subsequently performed, with no imaginary frequency results. The IEF-PCM (integral equation formalism - polarized continuum model) method was used in the solvent model with a dielectric constant set at ϵ = 78.39 and α = 1.28.[21]

In case of Ac-(Gly)$_3$-NHCH$_3$ and Ac-(L-Ala)$_3$-NHCH$_3$ the crystal calculations were carried out with the PBC (periodic boundary condition) tool of Gaussian03 at the B3LYP/6-31G(d)//RHF/3-21G level of theory.

For the di-, tetra-, hexa-, and octapeptides and their aggregates {For-(L-Ala)$_i$-NH$_2$}$_j$ where i = 2, 4, 6, 8,.. and j = 1, 2, 3, 4,..} starting conformations were chosen to represent the ideal conformations of β-pleated sheets for Extβ, DSAS, and DSPS (for further information on the conformations of the secondary structure elements please see ref 22). For V and VI the ideal conformation of α-helices was chosen as a starting structure. In the dimer more relative arrangements for the helices were tried, and the most stable, parallel arrangement (with an interhelical angle of 101°) was kept. As the dimer was also fully optimized, the interhelical angle was not constrained, either. For VII, IX, and VIII subsequent γ-turns were used, and in dimers the chains were placed parallel and antiparallel to each other. In I, II, III, and IV β- and γ-turns were combined with β-sheets. Although some more structures were tried, we did not use any "random" configuration. This has two explanations: first that we tried only those secondary structures that have intra- or intermolecular H-bonding, as this is thought to give stability to the protein backbone. Second, those secondary structural elements are thought to have high stability that occurs frequently in proteins, and we have used all such elements (α-helix, β-sheet, and β- and γ-turns). The structures resulting after optimization are described in more detail in Table S1.

For the calculation of Gibbs free energy we have computed not only the zero-point energy but also the electronic, translational, rotational, and vibrational contributions of the entropy. These entropic contributions were only included in the Gibbs free energy. However, it must be noted that by definition the electronic entropy is zero, as all molecules are ground state singlets. The translational entropy is the same for molecules having the same number of atoms (therefore for dimers and also for monomers). The rotational entropy depends on the shape of the molecules, and even though the molecules are different, their rotational entropies are nearly the same (it is 39 cal·mol^{-1}·K^{-1} for every dimer). Therefore the entropy difference between the models originates mainly from vibrational sources.

Results and Discussion

The folding of the *ext*ended single stranded β-sheet conformation, or Extβ, into alternative secondary structure elements followed by dimerization is shown in Figure 1A. The reference structure transition of the present comprehensive analysis is the total electronic energy decrease (ΔE) associated with the dimerization of two extended polypeptide chains, namely the formation of a *d*ouble *s*tranded *a*ntiparallel β-pleated *s*heet, or DSAS in short. For example, for tetrapeptides the dimerization of For-(L-Ala)$_4$-NH$_2$ into [For-(L-Ala)$_4$-NH$_2$]$_2$ (adopting β_1 conformation) is favored by −31.13 kcal·mol^{-1} at B3LYP/6-31G(d) level of theory, set to be 100%. Common secondary structure elements of peptides and proteins, such as α- or 3$_{10}$-helices, β-sheets, hairpines, β- and γ-turns, etc., are known to have inherent stability giving rise to the formation of the core of globular proteins. Thus, all the above and additional backbone folds were generated and allowed to form dimers, to compare their relative stability to that of DSAS. None of the usual secondary structure elements can form dimers as thermodynamically stable as the *d*ouble *s*tranded *p*arallel or *a*ntiparallel β-pleated *s*heet, DSPS or DSAS (Table 1 and Figure 1). This is well exemplified by the case of helices. Even though the dimerization of an α- or 3$_{10}$-helix is energy favored (V → VI), the overall stability gained is only (25 + 9)% of that of DSAS. In other words, a typical dimer formed by 3$_{10}$- or α-helices is about 66% less stable than the appropriate DSAS is.

Calculations repeated for longer polypeptides, namely for hexa- and octa-alanines, have resulted in a very similar stability picture (Table 1). The appropriate stability ratios (Figure 1A) related to hexa- and octapeptides support again the overwhelming stability of DSAS. For example, in the case of the

Table 1. Relative Stability[a] (ΔE in %) of a Folding (or Aggregation) Step as Function of the Lengths of the Polypeptide Chain (for a Graphical Representation of the Data Associated with Tetrapeptides, i = 4, see Figure 1)

	length of the polypetide chain, For-(L-Ala)$_i$-NH$_2$			
type of backbone structure transformation $X \rightarrow Y$[b]	i = 2 dipeptides	i = 4 tetrapeptides	i = 6 hexapeptides	i = 8 octapeptides
reference transition	**100%**[c]	**100%**	**100%**	**100%**
Extβ → DSAS				
Extβ → I	*26%*[d]	10%	31%[e]	24%
I → II	53%	56%	49%	61%
II → III	NA[f]	20%	2%	2%
III → IV	NA	25%	15%	12%
IV → **DSAS**	NA	9%	7%	5%
Extb → V	NA	9%	26%	39%
V → VI	NA	25%	17%	19%
VI → **DSAS**	NA	66%	57%	42%
Extb → VII	18%	22%	25%	27%
VII → VIII	79%	66%	60%	57%
VIII → **DSAS**	3%	12%	15%	16%
VII → IX	74%	53%	48%	45%
IX → DSPS	7%	19%	20%	19%
DSPS → **DSAS**	1%	6%	7%	9%

[a] The reference transformation is the dimerization of DSAS, from two isolated Extβ units (for more detailed, see Table S1). [b] $X \rightarrow Y$ stands either for a backbone conformational change or for a dimerization. [c] For the dimers of the different peptide conformers, [For-(Ala)$_i$-NH$_2$]$_2$, relative stability is provided in % with respect to that of the $\Delta E_{\text{Ext}\beta} \rightarrow \Delta E_{\text{DSAS}}$ transition as follows: 100% * |(ΔE_Z − 2 * $\Delta E_{\text{Ext}\beta}$)/($\Delta E_{\text{DSAS}}$ − 2 * $\Delta E_{\text{Ext}\beta}$)| for structure Z. [d] Percentage reflecting to destabilization (positive ΔE values) are all with italic type face [e] For the different conformers of a single stranded peptide model, [For-(Ala)$_i$-NH$_2$]$_1$, relative stability is provided in % with respect to that of the $\Delta E_{\text{Ext}\beta} \rightarrow \Delta E_{\text{DSAS}}$ transition as follows: 100% * |(ΔE_Z − $\Delta E_{\text{Ext}\beta}$)/($\Delta E_{\text{DSAS}}$ − 2 * $\Delta E_{\text{Ext}\beta}$)| for conformer Z. [f] Conformation transition not applicable for dipeptides

(17) Perczel, A.; Gaspari, Z.; Csizmadia, I. G. *J. Comput. Chem.* **2005**, *26*, 1155−1168.
(18) Pohl, G.; Beke, T.; Borbely, J.; Perczel, A. *J. Am. Chem. Soc.* **2006**, *128*, 14548−14559.
(19) Sawaya, M. R.; Sambashivan, S.; Nelson, R.; Ivanova, M. I.; Sievers, S. A.; Apostol, M. I.; Thompson, M. J.; Balbirnie, M.; Wiltzius, J. J. W.; McFarlane, H. T.; Madsen, A. O.; Riekel, C.; Eisenberg, D. *Nature* **2007**, *447*, 453−457.
(20) M. J. Frisch et. al. *Gaussian03*; Gaussian, Inc.: Wallingford, CT, 2004.
(21) Cossi, M.; Barone, V.; Mennucci, B.; Tomasi, J. *Chem. Phys. Lett.* **1998**, *286*, 253−260.
(22) Perczel, A.; Csizmadia, I. G. *THEOCHEM* **1993**, *105*, 75−85.

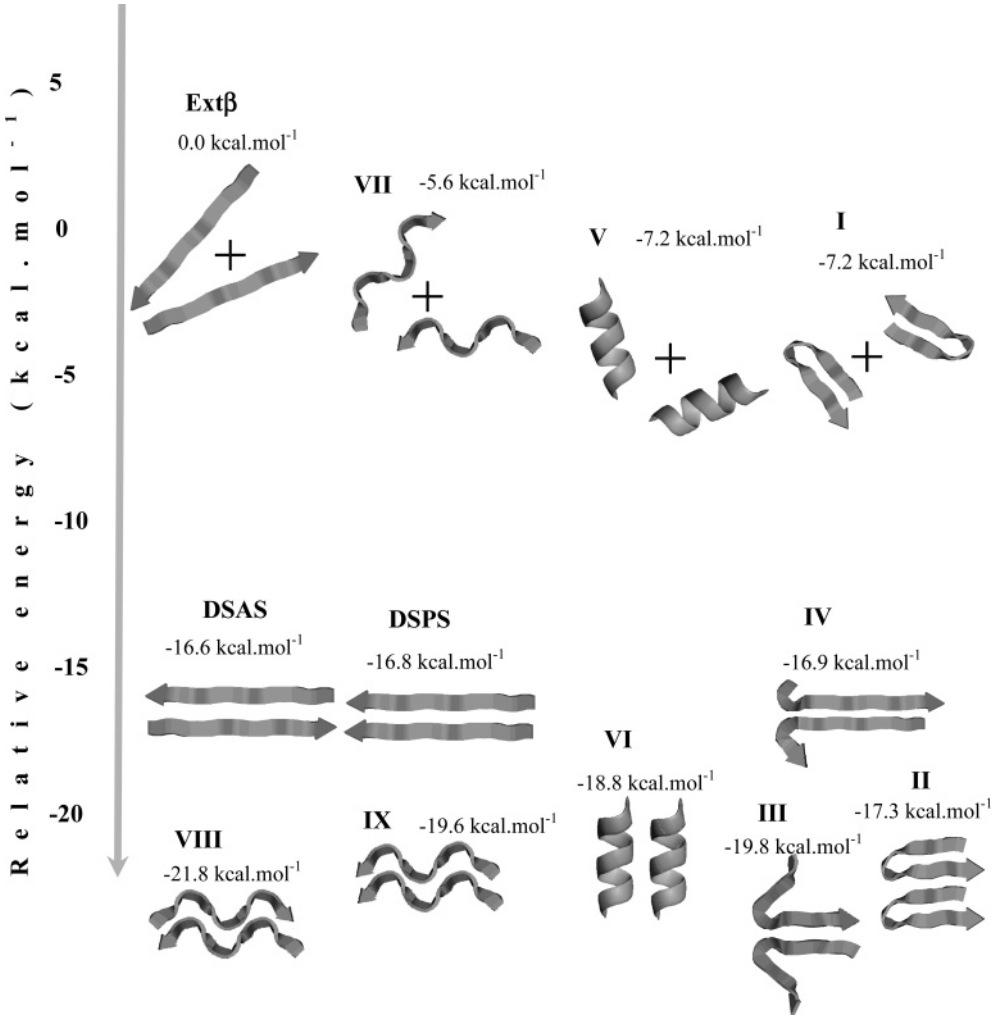

Figure 2. $T\Delta S$ (energy difference derived from entropy) of a folding or aggregation step of short polypeptides with respect to the Extβ units.

octapeptide models even the lowest energy dimers formed by 3_{10}-helices (VI → DSAS), parallel γ-turns (IX → DSAS), and antiprallel γ-turns (VIII → DSAS) are less stable than DSAS by 42%, (19 + 9)%, and 16%, respectively (Table 1). Thus, the elongation of the interacting backbones when forming different dimers is not expected to reshuffle their relative stability order.

The construction of a supramolecular system, dimerization and oligomerization of "monomers", increases order which results in information (I) accumulation within the system during aggregation ($I > I_0$ and $(I/I_0) > 1$), quantified by changes in entropy:[1]

$$\ln(I/I_0) = -(1/R)(S - S_0) = -(1/R)\Delta S \qquad (1)$$

The complexity may be conveniently defined as[2]

$$\text{complexity} = \text{RT} \ln(I/I_0) = -T\Delta S \qquad (2)$$

The necessary entropy and free energy data both can be obtained by frequency calculations (see Methods). The quantum chemically computed thermodynamic functions are *internal* or *intrinsic* values characteristic to an isolated single molecule. It does not include environmental interactions that may occur in the living cell. This is also the case of the entropy calculations. They yield *intrinsic* entropy values. It does not include randomly generated ensembles of molecules. However, this intrinsic entropy is a matching component of the intrinsic enthalpy and for the intrinsic Gibbs free energy values, computed quantum chemically. Consequently, the results of the present computations represent an important guide to what secondary structures, as such, represent in a thermodynamic sense. Although, the quantum chemical computations may well be regarded as exploratory in nature, nevertheless the conclusion is significant, at least at that level of theory.

All dimers composed of different secondary structure elements resulted in supramolecular complexes of equal or higher complexity than that of DSPS or DSAS (Figure 1B and Table S1). For example, the complexity of the dimers formed by 3_{10}-helices (VI), parallel γ-turns (IX), and antiprallel γ-turns (VIII) are about the same or slightly higher as computed for DSAS, namely 113%, 118%, and 130%, respectively (Table S1 and Figure 1B). Thus, all dimers investigated here contain about the same (or more) amount of complexity or "information" as DSAS (or DSAS) does. This holds for the monomers also. Therefore the contribution of entropy to the Gibbs free energy is in the same range for the monomers ($0 \rightarrow -7.2$ kcal·mol^{-1})(see Figure 2) and for the dimers (-16.5 kcal·mol$^{-1} \rightarrow -21.8$ kcal·mol^{-1}), giving the impression that it is not the entropy change that selects between conformers. Even so, the DSAS

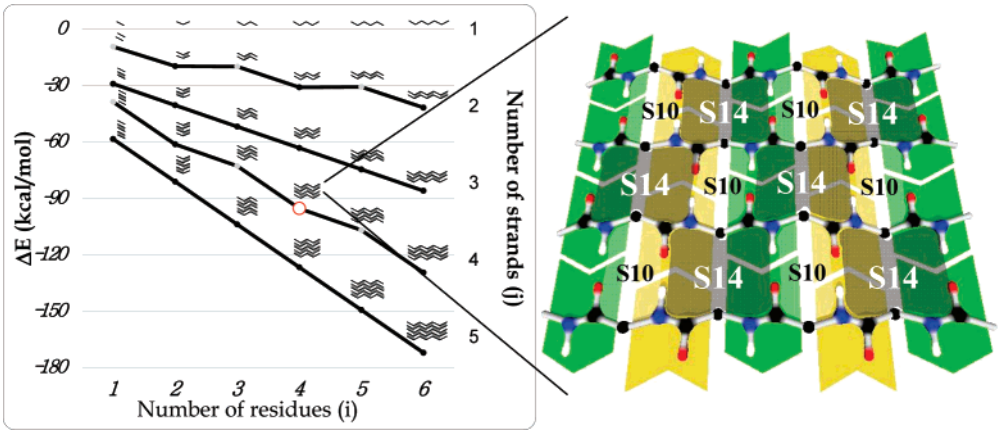

Figure 3. Total electronic stabilization effect (ΔE, kcal·mol^{-1}) of the interchain hydrogen-bond network. For multiple stranded β-layers formed by {For-(L-Ala)$_i$-NH$_2$}$_j$ at $j = 2, 3, 4$ the stability increases with the increase of the length of the polypeptide chain ($i = 1, 2, 3, 4, 5, 6$). All ΔEs are with respect to the isolated and independent Extβ conformers of {For-(L-Ala)$_i$-NH$_2$}$_j$ where $j = 1$ and $1 \leq i \leq 6$. The schematic diagram of a tetrapeptide tetramer arranged as a four-stranded antiparallel β-layer ($i = 4$, $j = 4$) is enlarged. The most stable S14 pseudo-rings are shaded, and the less stable S10 subunits are brighter. (Structures depicted by gray circles contain an odd number of S10 substructures providing less internal stability.) Both ΔH and ΔG functions show a highly similar profile (for data see Table S1).

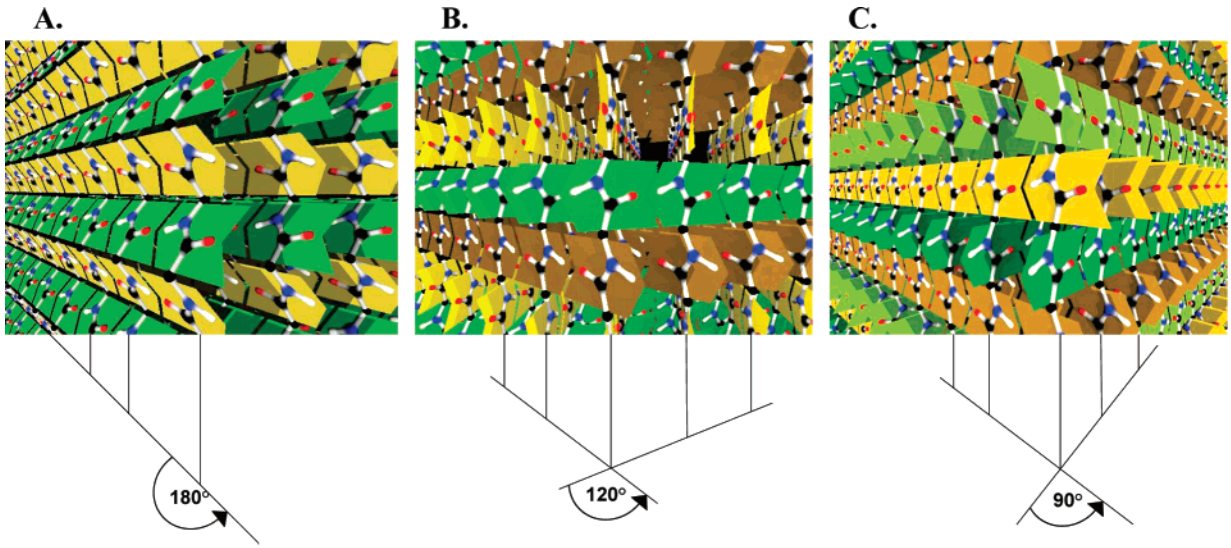

Figure 4. Schematic representation of the cross sections of the calculated nanoaggregates. (A) Multiple planes of 2D β-layers, thus 3D, with horizontal hydrogen bonds only between strands. (B) A 3D aggregate where the horizontal hydrogen bonds are heading toward three directions due to the 120° tilt angle of the adjacent amide planes in the backbone. (C) A 3D aggregate where the horizontal hydrogen bonds are heading toward four perpendicular directions due to the 90° tilt angle of the adjacent amide planes in the backbone.

Table 2. Measured and Computed Structural Parameters[a] of Ala Containing "Packed" β-Sheets

	measured SSTSAA peptide[b]	measured SNQNNF peptide[b]	computed (AAA)$_n$ peptide
$d_{H..O}$ (H-bond length)	3.06 ± 0.03	2.94 ± 0.13	2.81 ± 0.02
$d_{Ca..Ca}$ (distance between β-layers)	5.79 ± 0.33	7.60 ± 0.22	7.01 ± 0.0

[a] All values are in Å. [b] Sawaya et al.[19]

and DSPS have the smallest negative $T\Delta S$, meaning that the smallest part of their enthalpy is needed for increasing their complexity.

Therefore, the overall stability of double stranded β-strands measured in terms of free energy (ΔG) (Figure 1B and Table S1) is always the highest. For example, the relative stability expressed in Gibbs free energy for the dimers of double stranded antiparallel γ-turns (VIII) and parallel γ-turns (IX) with respect to that of DSAS is only 20% and 6%, respectively. Furthermore, ΔG values associated with the dimer of 3_{10}-helices (VI) indicates a strong destabilization: 86% ($\Delta G = +10.04$ kcal·mol^{-1}) (Table S1 and Figure 1B). Thus, unlike entropy, ΔH and consequently ΔG discriminate quite extensively between the different isolated or dimerized conformers, signaling unquestionably the overwhelming stability of both DSAS and DSPS.

Furthermore, stability calculations carried out by using a suitable solvent model, set up for an aqueous environment mimicking physiologic conditions of protein folding, have led to the same qualitative results resulting in again the outstanding stability of DSAS and DSPS (Table S1 and Figure S1). All monomer and dimer structures were fully optimized in a hydrated environment ($\epsilon = 78.39$). Even the lowest energy dimers formed by 3_{10}-helices (VI), double stranded parallel γ-turns (IX), and antiprallel γ-turns (VIII) are less stable than DSAS by 38%, (22 + 10)%, and 20%, respectively (Figure S1).

Table 3. Relative Stability of the Model Peptide Ac-$(Xxx)_n$-$NHCH_3$ as a Function of Tilt Angle, θ, in an Alternative Crystal-like 3D Packing[a]

	type of the lattice (structural properties of the aggregate)					
constitution of the building blocks $(Xxx)_3$	2D parallel β-layer, $q = 180°$	2D *anti*parallel β-layer, $q = 180°$	3D β-layer untilted: $q = 180°$	3D packing H-bonds tilted by $q = 60°$	3D packing H-bonds tilted by $q = 90°$	3D ϵ-layer H-bonds tilted by $q = 120°$ [c]
achiral (Xxx = Gly)	−0.16 (2%)[b]	−1.82 (21%)	−4.88 (55%)	0.0 (0%)[d]	−1.48 (17%)	−8.84 (100%)
chiral (Xxx = L-Ala)	−16.40 (93%)	−17.57 (100%)	−15.84 (90%)	−4.78 (27%)	−4.34 (25%)	0.0 (0%)[e]

[a] The appropriate tripeptide is periodically and endlessly repeated in the two-dimensional plane perpendicular to the polypeptide chain, yielding an "endless" 3D structure. [b] Relative energies are in kcal·mol^{-1}. Values in parentheses represent the relative percentage with respect to the most stable crystalline form. For [Ac-$(Gly)_3$-$NHCH_3$] the calculation of the relative stabilities is the following: $\Delta E_{\theta=x} = 100\%(E_{\theta=x} - E_{\theta=60})/(E_{\theta=60} - E_{\theta=120})$; for [Ac-$(Ala)_3$-$NHCH_3$]: $\Delta E_{\theta=x} = 100\%(E_{\theta=x} - E_{\theta=120})/(E_{\theta=120} - E_{\theta=180})$. [c] Hexagonal arrangement resulting in a polyproline II structure for the molecule. [d] $E = -872.599\ 781\ 4$ hartree. [e] $E = -990.523\ 442\ 6$ hartree.

In conclusion, both in vacuum and in aqueous media ΔE as well as ΔH and ΔG forecast the vast stability gained when DSAS or DSPS is formed with respect to any other dimer structures.

β-strands or cross-β structures[11] can be considered as aggregates of two, three, or multiple β-strands composed of very simple structural subunits designated as S10 and S14 for antiparallel (Figure 3) and S12 for parallel systems. These adjacent "lego" elements have different sizes and stabilities; S10 appears to be "neutral" while each S14 subunit adds an extra stability of approximately 10 kcal·mol^{-1} [23] to the molecular system. A single S12 unit stabilizes a parallel β-layer by some 7 kcal·mol^{-1}. The formation of antiparallel β-layers (e.g., ...-S10S14S10S14-..) implies that the S10 and S14 subunits are incorporated in an alternating fashion, while the formation of parallel β-layers means the incorporation of S12 units only. Due to the monotonically increasing number of favorable interactions between the polypeptide chains, the stability of the supramolecular system increases as the β-layer becomes longer and more extended for both the parallel and antiparallel supramolecular system. A similar type of stability analysis was conducted by calculating ΔH and ΔG measures for these complexes (Table S1) and found again that, with the increase of the length of the polypeptide chain as well as with the enlargement of the β-layer, incorporating a higher number of β-strands, the stability increases monotonically. The total energy of multiple stranded parallel β-layers of $\{For\text{-}(L\text{-}Ala)_i\text{-}NH_2\}_j$ where $i = 1, 2, 3, 4$, etc. and $j = 1, 2, 3, 4$, etc. decreases also in a very similar manner (data not shown) even though for selected oligomers one or two extra H-bonds may appear providing some surplus stability.

The optimum molecular packing of peptides in a crystal-like form has yet to be determined. This is to test *all* possible arrangements when peptide chains are oriented side-by-side and are interconnected by H-bonding. With respect to a *quasi* 2D β-layer where all interchain hydrogen bonds are within the β-layer (Figure 4A), tilting the angle of the adjacent amide planes by θ allows the formation of very compact 3D supramolecular aggregates (Figure 4B and C), as the H-bond network no longer remains in the "horizontal" or inherent plane. The 3D space can be endlessly filled by these repeated polypeptide subunits only if the tilt angle θ is any of 180°, 120°, 90°, or 60° (Figure 4 and Figure S2). In this manner in each aggregate, a peptide chain forms the same number of hydrogen bonds with all donor NHs and all acceptor COs of the backbone bonded.

The structural properties of the "AAA" [Ac-$(Ala)_3$-$NHCH_3$] crystal was compared to the "SSTSAA" and "SNQNNF" hexapeptide of Sawaya et al (Table 2).[19] The first was selected because its molecular arrangement in crystal is the same as the arrangement of "AAA" in our calculated crystal. The second was selected because it contains only small side chain residues and has an interface between Ala residues.[19] In the "SSTSAA" crystal, where multiple interactions between side chain atoms is possible, the distance between the β-layers is about 1.2 Å shorter than that computed for the oligoalanine model system. For the "SNQNNF" peptide the distance between the β-layers is 0.6 Å larger than that for the calculated AAA peptide, which can be due to the fact that the SNQNNF peptide possesses larger side chains. The measured H-bond lengths are a bit longer than our calculated ones; nevertheless the value for the "AAA" peptide stays in the error bar of the "SNQNNF" peptide. This indicates clearly that our computed "AAA" crystal has structural properties close to measured values.

The relative stability of tripeptides in endless crystal composed of either achiral glycines or chiral alanines was determined (Table 3). For achiral triglycines, [Ac-$(Gly)_3$-$NHCH_3$], the greatest stability is gained when $\theta = 120°$ (Figure 4B, Table 3, and Table S2).

In this form of crystalline packing the stability gained for an "endless" tripeptide with respect to its most unstable form, where $\theta = 60°$, is $\Delta E_{\theta=120°} = -8.84$ kcal·mol^{-1}. This most stable form is a superstructure where a molecule has a polyproline II like backbone conformation which was also described by Crick and Rich.[24] However, the endless crystalline packing in such a hexagonal form is only favored when the polypeptide has no side chains at all (R = H)!

For chiral peptides, which are typical of protein fragments, the hexagonal 3D arrangement described above (Figure 4B) becomes extremely disfavored. For these chiral systems, crystalline forms with horizontal H-bonds (where $\theta = 180°$) are the most preferred molecular arrangement (Table 3, Table S2, and Figure 3A), with the 2D antiparallel layer being the absolute minimum. The small relative stabilization energy difference between the two parallel crystalline packing arrangements with $\theta = 180°$, 2D layer and 3D layer ($\Delta\Delta E = 0.56$ kcal·mol^{-1}), suggest that when forming an amyloid-like 3D aggregate, chiral oligopeptides such as -$(L\text{-}Ala)_n$- with almost no interaction between the side chain groups (methyl for Ala) located in different β-layers is expected. However, it is likely that for side chains other than methyl (e.g., bulkier and more hydrophobic),

(23) Perczel, A.; Hudaky, P.; Fuzery, A. K.; Csizmadia, I. G. *J. Comput. Chem.* **2004**, *25*, 1084−1100.

(24) Crick, F. H. C., & Rich, A. Structure of polyglycine II. *Nature* **176**, 780−781 (1955)

more intensive layer−layer interactions might take place, which may provide a tighter molecular packing with further stabilization energy to the system, as described by Nelson et al.[2] and Sawaya et al.[19] for steric zippers.

Nevertheless, even for the smallest apolar side chain of Ala the β-layer with $\theta = 180°$ is selected, the prototype or "seed" of an amyloid-like aggregate.

Conclusion

In conclusion, we have shown that, among all the tested aggregates, two- or multiple-stranded β-sheets are the most stable secondary structure elements. Once the aggregation has started, there is no thermodynamic reason for it to stop. Therefore, a clear theoretical explanation is given here to the packed β-layers forming an amyloid-like aggregate. Also the existence of such an amyloid-like state is explained and why proteins take it up when interchain and 3D packing preferences jeopardize the globular fold. β-Pleated sheet preference seems to be a general feature of backbones that behave as polymers rather than proteins. This is the explanation why no primary sequence information encodes amyloid-like aggregation. Fortunately, nature uses alternative strategies[25−27] to prevent proteins from aggregating and preserve their native structure.[28] The insertion of "structural gatekeepers",[26] the use of domains of low (30−40%) sequence homology in multidomain proteins,[25] or the application of a "negative design" for protection of all free edge β-strands[27] seems essential to avoid protein aggregation. In this way forestalling deposition diseases that are energetically the "dead-ends" of protein folding becomes possible.

Acknowledgment. Dedicated to Professor Árpád Kucsman on the occasion of his 80th birthday. The help of Imre G. Csizmadia, Zoltán Gáspári, Tamas Fekete, William M. Westler, and Suzanne K. Lau is highly appreciated. We thank the supercomputing center of HAS-KFKI AEKI and HPC Szeged. This work was supported by grants from the Hungarian Scientific Research Fund (OTKA T047186, TS49812), MediChem2, Fullbright Fellowship and ICGEB (Hun04-03).

Supporting Information Available: Figure S1, Table S1, Figure S2, Table S2, and complete ref 20. This material is available free of charge via the Internet at http://pubs.acs.org.

JA0747122

(25) Wright, C. F.; Teichmann, S. A.; Clarke, J.; Dobson, C. M. *Nature* **2005**, *438*, 878−881.

(26) Otzen, D. E.; Kristensen, O.; Oliveberg, M. *Proc. Natl. Acad. Sci. U.S.A.* **2000**, *97*, 9907−9912.

(27) Richardson, J. S.; Richardson, D. C. *Proc. Natl. Acad. Sci. U.S.A.* **2002**, *99*, 2754−2759.

(28) Bucciantini, M.; Giannoni, E.; Chiti, F.; Baroni, F.; Formigli, L.; Zurdo, J. S.; Taddei, N.; Ramponi, G.; Dobson, C. M.; Stefani, M. *Nature* **2002**, *416*, 507−511.